



VIBRATION-BASED DIAGNOSTICS OF FATIGUE DAMAGE OF BEAM-LIKE STRUCTURES

V. V. MATVEEV AND A. P. BOVSUNOVSKY

*Department of Oscillations and Vibration Reliability, Institute for Problems of Strength,
National Academy of Sciences of Ukraine, Timiriazevskaia st.2, 01014 Kyiv, Ukraine.*

E-mail: bovs@ipp.adam.kiev.ua

(Received 31 October 2000, and in final form 27 March 2001)

The analytical investigation of vibration of damaged structures is a complicated problem. This problem may be simplified if a structure can be represented in the form of a beam with corresponding boundary and loading conditions. In this connection, free vibrations of an elastic cantilever Bernoulli–Euler beam with a closing edge transverse crack is considered in the present work as a model of a structure with a fatigue crack. The modelling of bending vibrations of a beam with a closing crack is realized based on the solutions for an intact beam and for a beam with an open crack. The algorithm of consecutive (cycle-by-cycle) calculation of beam mode shapes amplitudes is presented. It is shown that at the instant of crack opening and closing, the growth of the so-called concomitant mode shapes which differ from the initially given mode shape takes place. Moreover, each of the half-cycles is characterized by a non-recurrent set of amplitudes of concomitant modes of vibration and these amplitudes are heavily dependent on the crack depth.

The vibration characteristics of damage based on the estimation of non-linear distortions of the displacement, acceleration and strain waves of a cracked beam are investigated, and the comparative evaluation of their sensitivity is carried out.

© 2002 Academic Press

1. INTRODUCTION

Many mechanical structures in real service conditions are subjected to combined or separate effects of the dynamic load, temperature and corrosive medium, with a consequent growth of fatigue cracks, corrosive cracking and other types of damage. The immediate visual detection of damage is difficult or impossible in many cases and the use of local non-destructive methods of damage detection requires time and financial expense and frequently is inefficient.

In this connection, the use of vibration methods of damage diagnostics is promising. These methods are based on the relationships between the vibration characteristics (natural frequencies [1–3] and mode shapes [4]) or peculiarities of a non-linear vibration system behaviour (for example, non-linear distortions of the displacement wave in different cross-sections of a beam [5, 6], the amplitudes of sub-resonance and super-resonance vibrations [7], the anti-resonance frequencies [8], etc.) and damage parameters. It is important to note that the essential non-linearity of vibrations of a body with a fatigue crack is due to the change of stiffness at the instant of crack opening and closing and is the main difficulty in the solution of such class problems.

The analytical investigation of vibrations of damaged structures is a complicated problem. This problem may be simplified if a structure can be represented in the form of

a beam with corresponding boundary and loading conditions. This class of structures can include bridges, offshore platforms, pipelines, masts of electricity transmission, TV towers, aircraft wings, blades and rotors of turbine engines, propellers of helicopters and many others.

In earlier work [9], the solution of the problem of the bending vibrations of a cantilever beam with a closing crack during the first cycle of vibration was described. It was shown that at the instant of crack opening, the so-called concomitant mode shapes differ from the initially given mode shape. This approach to the solution of the problem can be extended not only over the first but also over the subsequent cycles.

The present work is a logical continuation of that research [9]. Therefore, the aim of the study is to develop the algorithm of consecutive (cycle-by-cycle) calculation of cracked beam mode shapes amplitudes, to investigate the regularities of concomitant mode shapes origination, and to study the level of non-linear distortions of the displacement, acceleration and strain waves.

2. MODELLING OF VIBRATION OF A BEAM WITH A CLOSING CRACK

The modelling of free bending vibrations of a beam with a closing crack is based on the solutions for an intact beam and for a beam with an open crack [9].

Free bending vibrations of a beam neglecting the damping effect are described by the differential equation:

$$\frac{\partial^4 y(x, t)}{\partial x^4} + \frac{\rho A}{EI} \frac{\partial^2 y(x, t)}{\partial t^2} = 0. \quad (1)$$

where E and ρ are the Young's modulus and the density of the beam material respectively, $I = bh^3/12$ and $A = bh$ are the moment of inertia and area of the cross-section respectively, b and h are the width and height of cross-section respectively.

The general solution of equation (1) can be presented in the following form:

$$y(x, t) = \sum_{i=1}^{\infty} w_i(x) (P_i \sin \omega_i t + R_i \cos \omega_i t), \quad (2)$$

where $w_i(x)$ and ω_i are the mode shapes and natural angular velocities respectively, and i is the number of the mode shape. The mode shapes of the beam are described by the expression

$$w_i(x) = A_i S(k_i x) + B_i T(k_i x) + C_i U(k_i x) + D_i V(k_i x), \quad (3)$$

where $k_i^4 = \omega_i^2 \rho A / EI$; $S(k_i x)$, $T(k_i x)$, $U(k_i x)$, $V(k_i x)$ are the Krylov functions [9]. Coefficients A_i , B_i , C_i and D_i in expression (3) are determined from the boundary conditions for the cantilever beam (Figure 1):

$$w_i(0) = 0, \quad \theta_i(\theta) = \frac{\partial w_i(0)}{\partial x} = 0, \quad M_i(L) = I_m \omega_i^2 \frac{\partial w_i(L)}{\partial x}, \quad Q_i(L) = -m_L \omega_i^2 w_i(L), \quad (4)$$

where $\theta(x)$ is the angle of rotation of the cross-section x , $M(x)$ is the bending moment, $Q(x)$ is the transverse force, L is the length of the beam, m_L is the mass on the end, and I_m is the moment of inertia of the mass.

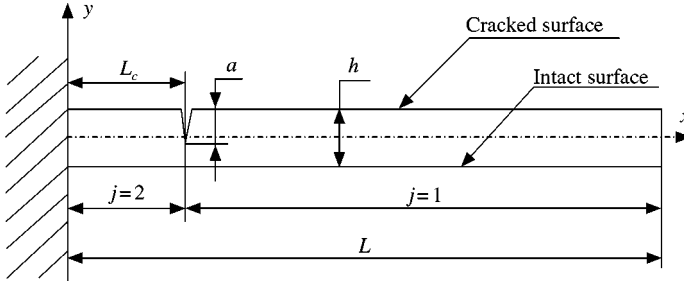


Figure 1. Geometry of a cantilever beam with an edge closing crack.

The characteristic equation in this case assumes the form

$$[S(k_i L) - qT(k_i L)] [S(k_i L) + gV(k_i L)] - [T(k_i L) - qU(k_i L)] [V(k_i L) + gU(k_i L)] = 0, \quad (5)$$

where $q = I_m k_i^3 / \rho A$, and $g = m_L k_i / \rho A$.

As distinct from reference [9], a beam with an open-edge crack is modelled here by two sections connected by means of the cross-section with an increased compliance [10] located at a distance L_c from the clamped end. Free bending vibrations of each section neglecting the damping effect are described by the differential equation (1) in which $I = I_j$ is the cross-sectional moment of inertia of the section number j ($j = 1, 2$). In this case, $I_1 = I_2 = I$. The general solution of equation (1) for the section number j takes the form

$$y_{oj}(x, t) = \sum_{i=1}^{\infty} w_{ij}(x) (P_{oi} \sin \omega_{oi} t + R_{oi} \cos \omega_{oi} t), \quad (6)$$

where

$$w_{ij}(x) = A_{ij} S(k_{ij} x) + B_{ij} T(k_{ij} x) + C_{ij} U(k_{ij} x) + D_{ij} V(k_{ij} x) \quad (7)$$

are the mode shapes of the section number j , $k_{ij}^4 = \omega_{oi}^2 \rho A / EI_j$, and ω_{oi} is the natural angular velocity of a beam with an open crack (subscript “o” signifies an open crack). From expression (7) with the boundary conditions in equation (4) the functions describing the angle of rotation $\theta_{ij}(x)$, bending moment $M_{ij}(x)$ and transverse force $Q_{ij}(x)$ can be derived.

The boundary conditions at the clamped end ($x = 0$) and free end ($x = L$) of the beam and conditions of compatibility of sections 1 and 2 ($x = L_c$) will be [10]

$$w_{i2}(0) = 0, \quad \theta_{i2}(0) = 0,$$

$$M_{i1}(L) = I_m \omega_{oi}^2 k_{oi} [A_{i1} V(k_{oi} L) + B_{i1} S(k_{oi} L) + C_{i1} T(k_{oi} L) + D_{i1} U(k_{oi} L)],$$

$$Q_{i1}(L) = -m_L \omega_{oi}^2 [A_{i1} S(k_{oi} L) + B_{i1} T(k_{oi} L) + C_{i1} U(k_{oi} L) + D_{i1} V(k_{oi} L)],$$

$$w_{i1}(L_c) = w_{i2}(L_c), \quad \theta_{i1}(L_c) - \theta_{i2}(L_c) = \delta_c M_{i1}(L_c), \quad M_{i1}(L_c) = M_{i2}(L_c), \quad Q_{i1}(L_c) = Q_{i2}(L_c),$$

where δ_c is the change of compliance of the cross-section with the crack.

Taking into consideration the fact that $S(0) = 1$, $T(0) = U(0) = V(0) = 0$ and the first two boundary conditions, it can be shown that $A_{i2} = B_{i2} = 0$. Residuary boundary and

compatibility conditions determine the set of equations, the determinant of which takes the form

$$\begin{vmatrix} U(\varphi_i) - q_o V(\varphi_i) & V(\varphi_i) - q_o S(\varphi_i) & S(\varphi_i) - q_o T(\varphi_i) & T(\varphi_i) - q_o U(\varphi_i) & 0 & 0 \\ T(\varphi_i) - g_o S(\varphi_i) & U(\varphi_i) + g_o T(\varphi_i) & V(\varphi_i) + g_o U(\varphi_i) & S(\varphi_i) + g_o V(\varphi_i) & 0 & 0 \\ S(\psi) & T(\psi) & U(\psi) & V(\psi) & -S(\psi) & -T(\psi) \\ V(\psi_i) - r_o U(\psi_i) & S(\psi_i) - r_o V(\psi_i) & T(\psi_i) - r_o S(\psi_i) & U(\psi_i) - r_o T(\psi_i) & -T(\psi) & -U(\psi) \\ U(\psi) & V(\psi) & S(\psi) & T(\psi) & -S(\psi) & -T(\psi) \\ T(\psi) & U(\psi) & V(\psi) & S(\psi) & -V(\psi) & -S(\psi) \end{vmatrix} = 0, \quad (8)$$

where $\varphi_i = k_{oi}L$, $\psi_i = L_c\varphi_i/L$, $q_o = I_m\varphi_i^3/\rho AL^3$, $g_o = m_L\varphi_i/\rho AL$, and $r_o = EI\delta_c\varphi_i/L$.

The solution of the characteristic equation (8) and of the set of equations determines the natural frequencies and mode shapes of the beam with an open crack (it is accepted here that $M_{i2}(0) = M(0)$).

The compliance of the cross-section with a crack is determined using linear fracture mechanics. In the linear elastic body, the change of strain energy due to crack presence of the mode I deformation with the assumption of plane stress will be as follows [11]:

$$\Delta U = \frac{b}{E} \int_0^a K_1^2 d\alpha, \quad (9)$$

where a is the crack depth. At the same time, the change of strain energy in the cracked cross-section can be expressed via the change of its compliance:

$$\Delta U = 0.5\delta_c M^2. \quad (10)$$

Here, the expression for the stress intensity factor (SIF) obtained by Cherepanov for the case of pure bending of a cracked strip [12] is used as

$$K_I = \frac{4.2 M}{bh^{3/2}} [(1 - \gamma)^{-3} - (1 - \gamma)^3]^{1/2}, \quad (11)$$

where $\gamma = a/h$. Using equations (9) and (10) with equation (11) gives

$$\delta_c(\gamma) = \frac{8.82 [(1 - \gamma)^6 - 3(1 - \gamma)^2 + 2]}{(1 - \gamma)^2 bh^2 E} \quad (12)$$

It is interesting to note that the results of calculations of natural frequencies and mode shapes (up to and including five modes) for a cantilever beam with the model of the crack presented here and with a more complicated model of the crack in the form of a short section with the reduced moment of inertia of the cross-section [9] were found to be the same. In both cases equation (11) was applied. If use is made of other equations for the SIF, then the results for the natural frequencies and mode shapes will be different insofar as the SIF values will be different. For example, the discrepancy between the SIF values calculated by the formulae from reference [13] and equation (11) reaches 13.2%. Thus, the justification of modelling vibration of a cracked beam if the energy approach is used depends mainly on the choice of expression for the SIF and practically does not depend on the type of crack model. The preference given here for equation (11) was justified earlier [9].

The beam with a closing crack is modelled in the following way: at the half-cycles while the crack is closed, the vibrations of the beam are described by equation (2) (it is presumed that the stiffness of the intact beam and the stiffness of the beam with a closed crack are

equal); at the half-cycles while the crack is open, the vibrations of the beam are described by equation

$$y_{cj}(x, t) = \sum_{i=1}^{\infty} w_{ij}(x)(P_{ci} \sin \omega_{oi}t + R_{ci} \cos \omega_{oi}t), \quad (13)$$

which differs from equation (6) only by the coefficients of mode shapes P_{ci} and R_{ci} (subscript "c" signifies the closing crack).

Coefficients P_i and R_i in equation (2) and P_{ci} and R_{ci} in equation (13) are determined from the initial conditions for the displacement, velocity and angle of rotation at a certain instant of time with mode shape orthogonality (for details see reference [9]):

$$\int_0^L m w_s(x) w_i(x) dx + m_L w_s(L) w_i(L) + I_m \theta_s(L) \theta_i(L) = 0.$$

It is assumed that on the first and subsequent odd half-cycles ($n = 1, 3, 5, \dots$) the crack is closed and on the even half-cycles ($n = 2, 4, 6, \dots$) it is open. Initial conditions for displacement, velocity, and angle of rotation of the cross-section and its velocity variation on the first half-cycle ($n = 1$) at the instant of time $t_1 = 0$ have, respectively, the appearance: $y_1(x) = 0$, $v_1(x) = \omega_s w_s(x)$, $\theta_1(L) = 0$, $[\partial \theta_1(L, t) / \partial t]_{t_1=0} = \omega_s \theta_s(L)$, where s is the initial (main) mode shape. Other mode shapes ($i \neq s$) arising at the instant of crack opening or closing are denoted as concomitant. It is obvious that under the above-mentioned initial conditions $P_{1,s} = 1$ and $P_{1,i \neq s} = R_{1,i \neq s} = 0$.

On the even half-cycles of vibrations, the coefficients of mode shapes $P_{n,ci}$ and $R_{n,ci}$ are determined by the formulae

$$P_{n,ci} = \frac{[\omega_{oi} G_{n,1} \sin \omega_{oi} t_n + G_{n,2} \cos \omega_{oi} t_n]}{\omega_{oi} [\int_0^{L_c} m w_{i2}^2(x) dx + \int_{L_c}^L m w_{i1}^2(x) dx + m_L w_{i1}^2(L) + I_m \theta_{i1}^2(L)]}, \quad (14)$$

$$R_{n,ci} = \frac{[\omega_{oi} G_{n,1} \sin \omega_{oi} t_n - G_{n,2} \cos \omega_{oi} t_n]}{\omega_{oi} [\int_0^{L_c} m w_{i2}^2(x) dx + \int_{L_c}^L m w_{i1}^2(x) dx + m_L w_{i1}^2(L) + I_m \theta_{i1}^2(L)]}, \quad n = 2, 4, 6, \dots, \quad (15)$$

where $m = \rho A$ is the beam mass per unit length,

$$G_{n,1} = \int_0^{L_c} m y_{n-1}(x) w_{i2}(x) dx + \int_{L_c}^L m y_{n-1}(x) w_{i1}(x) dx + m_L y_{n-1}(L) w_{i1}(L) + I_m \theta_{n-1}(L) \theta_{i1}(L),$$

$$G_{n,2} = \int_0^{L_c} m v_{n-1}(x) w_{i2}(x) dx + \int_{L_c}^L m v_{n-1}(x) w_{i1}(x) dx + m_L v_{n-1}(L) w_{i1}(L)$$

$$+ I_m \left[\frac{\partial \theta_{n-1}(L, t)}{\partial t} \right]_{t_n} \theta_{i1}(L)$$

under respective initial conditions

$$y_{n-1}(x) = \sum_{i=1}^{\infty} w_i(x)(P_{n-1,i} \sin \omega_i t_n + R_{n-1,i} \cos \omega_i t_n),$$

$$v_{n-1}(x) = \sum_{i=1}^{\infty} \omega_i w_i(x)(P_{n-1,i} \cos \omega_i t_n - R_{n-1,i} \sin \omega_i t_n),$$

$$\theta_{n-1}(L) = \sum_{i=1}^{\infty} \theta_i(L)(P_{n-1,i} \sin \omega_i t_n + R_{n-1,i} \cos \omega_i t_n),$$

$$\left[\frac{\partial \theta_{n-1}(L, t)}{\partial t} \right]_{t_n} = \sum_{i=1}^{\infty} \omega_i \theta_i(L)(P_{n-1,i} \cos \omega_i t_n - R_{n-1,i} \sin \omega_i t_n),$$

at the instants of time

$$t_n = \frac{n}{2} \frac{\pi}{\omega_s} + \left(\frac{n-2}{2} \right) \frac{\pi}{\omega_{os}}. \quad (16)$$

On the third and subsequent odd half-cycles of vibrations, the coefficients of mode shapes $P_{n,i}$ and $R_{n,i}$ are determined by the formulae

$$P_{n,i} = \frac{[\omega_i G_{n,3} \sin \omega_i t_n + G_{n,4} \cos \omega_i t_n]}{\omega_i \left[\int_0^L m w_i^2(x) dx + m_L w_i^2(L) + I_m \theta_i^2(L) \right]}, \quad (17)$$

$$R_{n,i} = \frac{[\omega_i G_{n,3} \sin \omega_i t_n + G_{n,4} \cos \omega_i t_n]}{\omega_i \left[\int_0^L m w_i^2(x) dx + m_L w_i^2(L) + I_m \theta_i^2(L) \right]}, \quad n = 3, 5, 7, \dots, \quad (18)$$

where

$$G_{n,3} = \int_0^L m y_{n-1,j}(x) w_i(x) dx + m_L y_{n-1,j}(L) w_i(L) + I_m \theta_{n-1,j}(L) \theta_i(L),$$

$$G_{n,4} = \int_0^L m v_{n-1,j}(x) w_i(x) dx + m_L v_{n-1,j}(L) w_i(L) + I_m \left[\frac{\partial \theta_{n-1,j}(L, t)}{\partial t} \right]_{t_n} \theta_i(L),$$

under respective initial conditions

$$y_{n-1,j}(x) = \sum_{i=1}^{\infty} w_{i,j}(x) (P_{n-1,ci} \sin \omega_{oi} t_n + R_{n-1,ci} \cos \omega_{oi} t_n),$$

$$v_{n-1,j}(x) = \sum_{i=1}^{\infty} \omega_{oi} w_{i,j}(x) (P_{n-1,ci} \cos \omega_{oi} t_n - R_{n-1,ci} \sin \omega_{oi} t_n),$$

$$\theta_{n-1,j}(L) = \sum_{i=1}^{\infty} \theta_{ij}(L) (P_{n-1,ci} \sin \omega_{oi} t_n + R_{n-1,ci} \cos \omega_{oi} t_n),$$

$$\left[\frac{\partial \theta_{n-1,j}(L, t)}{\partial t} \right]_{t_n} = \sum_{i=1}^{\infty} \omega_{oi} \theta_{ij}(L) (P_{n-1,ci} \cos \omega_{oi} t_n - R_{n-1,ci} \sin \omega_{oi} t_n),$$

at the instants of time

$$t_n = \frac{n-1}{2} \left(\frac{\pi}{\omega_s} + \frac{\pi}{\omega_{os}} \right). \quad (19)$$

The coefficients of mode shapes for the odd and even half-cycles as well as the vibration values averaged over N (even number) cycles were calculated by the formulae:

$$H_{n,i} = \sqrt{P_{n,i}^2 + R_{n,i}^2}, \quad H_{n,ci} = \sqrt{P_{n,ci}^2 + R_{n,ci}^2}, \quad (20)$$

$$\bar{H}_i = \frac{\sum_{n=1,3,\dots}^{N-1} H_{n,i}}{N}, \quad \bar{H}_{ci} = \frac{\sum_{n=2,4,\dots}^N H_{n,ci}}{N}. \quad (21)$$

In addition to the coefficients (20), their maximal ($H_{n,i}^{max}$, $H_{n,ci}^{max}$) and minimal ($H_{n,i}^{min}$, $H_{n,ci}^{min}$) values over N cycles were determined.

3. CRITERION FOR APPLICABILITY OF THE THEORY

The theory presented above is valid if the crack at the corresponding half-cycles is either permanently open or closed. However, when concomitant modes of vibration arise this

TABLE 1

Coefficients of the main and concomitant mode shapes for the beam with the crack location $L_c/L = 0.1$

a/h	s	i	$H_{n,i}^{min}/H_{n,ci}^{min}$	\bar{H}_i/\bar{H}_{ci}	$H_{n,i}^{max}/H_{n,ci}^{max}$
0.53	1	1	0.969/0.754	0.985/0.765	1.0/0.778
		2	0/0.016	0.141/0.106	0.231/0.167
		3	0/0.002	0.036/0.031	0.063/0.054
0.54	2	1	0/0.020	0.223/0.156	0.437/0.279
		2	0.782/0.569	0.921/0.644	1.0/0.694
		3	0/0.071	0.175/0.142	0.380/0.299
0.48	3	1	0/0.004	0.210/0.162	0.367/0.272
		2	0/0.005	0.203/0.158	0.437/0.342
		3	0.818/0.695	0.913/0.778	1.0/0.850

requirement is not always fulfilled. The permanence of the sign of the bending moment serves as a criterion for applicability of the theory, which is calculated at the cracked cross-section by the formulae

$$M_n(L_c, t) = \sum_{i=1}^{\infty} \left[\frac{\partial^2 w_i(x)}{\partial x^2} \right]_{x=L_c} (P_{n,i} \sin \omega_i t + R_{n,i} \cos \omega_i t), \quad (22)$$

$$M_{n,c}(L_c, t) = \sum_{i=1}^{\infty} \left[\frac{\partial^2 w_{i1}(x)}{\partial x^2} \right]_{x=L_c} (P_{n,ci} \sin \omega_{oi} t + R_{n,ci} \cos \omega_{oi} t). \quad (23)$$

Equation (22) is used on the odd half-cycles and equation (23) on the even half-cycles.

The relative crack depths shown in Table 1 are the upper limits of the theory's applicability range obtained by the above criterion for the three mode shapes of the cracked cantilever beam ($L/h = 20$, $b/h = 1$, $m_L = 0$) with the crack location at $L_c/L = 0.1$. These values of relative crack depth were used in calculations, the results of which are also indicated in Table 1. The results of calculations make it possible to conclude that each of the half-cycles is characterized by a non-recurrent set of amplitudes of concomitant modes of vibration and also that these amplitudes may reach substantial value; up to 44% of the amplitude of main mode (see last column in Table 1). The amplitudes of concomitant modes of the beam at the crack location $L_c/L = 0.5$ at the upper limits of the relative crack depths ($\gamma = 0.43$ for the first mode, $\gamma = 0.68$ for the second mode, $\gamma = 0.30$ for the third mode) were lower than in the case at $L_c/L = 0.1$.

It is necessary to note that the theory may be extended to the cases when the crack opens and closes more than once over a half-cycle but it is evident that the procedure of vibration simulation will become seriously complicated.

When the concomitant modes of vibration arise, the instants of time when the cracked cross-section is in the neutral position would not coincide with the corresponding instants of time determined by formulae (16) and (19). Therefore, for a numerical implementation of the theory, the calculation of the actual instants of time for the determination of initial conditions was arranged. As the investigations showed, the difference between these instants of time and those determined by formulae (16) and (19) was found to be negligible in the range of relative crack depth $0 \leq \gamma \leq 0.25$ as was the influence of this difference on the coefficients of mode shapes.

4. VIBRATION CHARACTERISTICS OF A BEAM WITH A CLOSING CRACK

The experimental verification [9] showed that the theory presented here makes it possible to predict the change of natural frequencies and mode shapes of a cantilever beam with a fatigue crack with sufficient accuracy. Furthermore, the testing of cracked specimens [14] revealed that the first-mode vibrations of the specimens with fatigue cracks was accompanied by the concomitant high modes of vibrations and that each cycle of vibration was characterized by a non-recurrent set of high modes. Consequently, the theory proposed here adequately describes the vibrations of a beam with a closing crack and can be used for investigations of different vibration characteristics of damage (VCD).

Subsequent investigations were restricted to the range of the relative crack depth $0 \leq \gamma \leq 0.25$ which is most interesting from the practical point of view. In this range of the relative crack depth, the maximal and minimal amplitudes of the main and concomitant modes of vibration and their values averaged over N cycles converge sufficiently fast to certain magnitudes, when the vibrations are steady state. This conclusion is illustrated by the results of calculation of the mode shapes coefficients $H_{n,i}$ and $H_{n,ci}$ ($L/h = 20$, $L_c/L = 0.1$, $\gamma = 0.25$, $m_L = 0$) and their averaged values (Tables 2–4). As can be seen, beyond the 25th cycle of vibration they are practically invariable. The deviations of coefficients $H_{n,i}$ and $H_{n,ci}$ for the main mode shapes from their averaged values are not shown in Tables 2–4 in

TABLE 2

Coefficients of the first main and concomitant mode shapes for the beam ($a/h = 0.25$, $L_c/L = 0.1$)

N	s = 1		i = 2		i = 3		
	\bar{H}_s/\bar{H}_{cs}	$H_{n,i}^{min}/H_{n,ci}^{min}$	\bar{H}_i/\bar{H}_{ci}	$H_{n,i}^{max}/H_{n,ci}^{max}$	$H_{n,i}^{min}/H_{n,ci}^{min}$	\bar{H}_i/\bar{H}_{ci}	$H_{n,i}^{max}/H_{n,ci}^{max}$
1	1.0/0.957	0/0	0/0.008	0/0.008	0/0	0/0.001	0/0.001
5	1.0/0.957	0/0.005	0.008/0.010	0.014/0.015	0/0.001	0.004/0.005	0.008/0.008
25	1.0/0.957	0/0.002	0.009/0.010	0.015/0.015	0/0.001	0.007/0.007	0.011/0.010
50	1.0/0.957	0/0.002	0.009/0.010	0.015/0.015	0/0.001	0.007/0.006	0.011/0.010
100	1.0/0.957	0/0.002	0.009/0.010	0.015/0.015	0/0.001	0.007/0.006	0.011/0.010
200	1.0/0.957	0/0.002	0.009/0.010	0.015/0.015	0/0.001	0.007/0.006	0.011/0.010

TABLE 3

Coefficients of the second main and concomitant mode shapes for the beam ($a/h = 0.25$, $L_c/L = 0.1$)

N	s = 2		i = 1		i = 3		
	\bar{H}_s/\bar{H}_{cs}	$H_{n,i}^{min}/H_{n,ci}^{min}$	\bar{H}_i/\bar{H}_{ci}	$H_{n,i}^{max}/H_{n,ci}^{max}$	$H_{n,i}^{min}/H_{n,ci}^{min}$	\bar{H}_i/\bar{H}_{ci}	$H_{n,i}^{max}/H_{n,ci}^{max}$
1	1.0/0.932	0/0	0/0.008	0/0.008	0/0	0/0.005	0/0.005
5	1.0/0.932	0/0.008	0.023/0.024	0.036/0.033	0/0.002	0.003/0.004	0.004/0.006
25	1.0/0.932	0/0.002	0.023/0.022	0.036/0.033	0/0.002	0.005/0.006	0.009/0.011
50	1.0/0.932	0/0	0.023/0.021	0.036/0.033	0/0.001	0.005/0.006	0.009/0.011
100	1.0/0.931	0/0	0.023/0.021	0.036/0.033	0/0.001	0.005/0.006	0.009/0.011
200	1.0/0.931	0/0	0.023/0.021	0.036/0.033	0/0.001	0.005/0.006	0.009/0.011

TABLE 4

Coefficients of the third main and concomitant mode shapes for the beam ($a/h = 0.25$, $L_c/L = 0.1$)

N	s = 3		i = 1		i = 2		
	\bar{H}_s/\bar{H}_{cs}	$H_{n,i}^{min}/H_{n,ci}^{min}$	\bar{H}_i/\bar{H}_{ci}	$H_{n,i}^{max}/H_{n,ci}^{max}$	$H_{n,i}^{min}/H_{n,ci}^{min}$	\bar{H}_i/\bar{H}_{ci}	$H_{n,i}^{max}/H_{n,ci}^{max}$
1	1.0/0.957	0/0	0/0.001	0/0.001	0/0	0/0.005	0/0.005
5	1.0/0.957	0/0.001	0.005/0.006	0.010/0.010	0/0.003	0.006/0.007	0.010/0.010
25	1.0/0.956	0/0.001	0.009/0.009	0.015/0.014	0/0.001	0.007/0.006	0.011/0.010
50	1.0/0.956	0/0.001	0.010/0.009	0.015/0.014	0/0.001	0.007/0.006	0.011/0.010
100	1.0/0.956	0/0	0.010/0.009	0.015/0.014	0/0.001	0.007/0.006	0.011/0.010
200	1.0/0.955	0/0	0.010/0.009	0.015/0.014	0/0	0.007/0.006	0.011/0.010

as much as they do not exceed 0.02% for the first, 0.17% for the second and 0.22% for the third mode shape.

Thus, in this case we can restrict the investigations to only the first cycle of vibration inasmuch as in the range $0 \leq \gamma \leq 0.25$, the difference between the main modes amplitudes of the first cycle and subsequent cycles lies within the boundaries of $\pm 0.22\%$. In addition, from these results it follows that in this case, the effect of concomitant modes of vibration on the vibration characteristics can be neglected by virtue of the smallness of their amplitudes on the first as well as on the subsequent cycles of vibration. Therefore, equations (2) and (13) are transformed into the form

$$y(x, t) = w_s(x) \sin \omega_s t; \quad (24)$$

$$y_{cj}(x, t) = w_{sj}(x) (P_{cs} \sin \omega_{os} t + R_{cs} \cos \omega_{os} t). \quad (25)$$

As in this case the effect of concomitant modes of vibration is neglected, the maximal deflection of the beam main mode of vibration on the first half-cycle ($n = 1$) will occur at the moment of time $t = t_2/2$, and on the second half-cycle ($n = 2$), at the moment $t = (t_2 + t_3)/2$. Taking into account formulae (16) and (17) and equations (24) and (25) the maximal deflections of the beam on different half-cycles is determined in the following way:

$$y^{max}(x) = w_s(x), \quad (26)$$

$$y_{cj}^{max}(x) = w_{sj}(x) \left(P_{cs} \cos \frac{\omega_{os}}{\omega_s} \pi - R_{cs} \sin \frac{\omega_{os}}{\omega_s} \pi \right). \quad (27)$$

The strain wave shape on the surface of the beam is described by equations:

$$\varepsilon(x, t) = M_s(x) \sin \omega_s t, \quad (28)$$

$$\varepsilon_c(x, t) = f_\varepsilon(x, \gamma) M_{sj}(x) (P_{cs} \sin \omega_{oi} t + R_{cs} \cos \omega_{oi} t), \quad (29)$$

where function $f_\varepsilon(x, \gamma)$ takes into account the effect of the crack on the strain distribution along the cracked and crack-free (intact) surfaces of the beam (see Figure 1). On the cracked side surface of the beam function $f_\varepsilon(x, \gamma)$ has the appearance [9]

$$f_\varepsilon(x, \gamma) = 1 - \exp[-h^{-1}|x - L_c|(1.366 + 0.304\gamma^{-1})]$$

and opposite to the cracked side surface of the beam:

$$f_{\varepsilon}(x, \gamma) = 1 + [\beta(\gamma) - 1] \exp[-h^{-2}(L_c - x)^2(0.063 + 0.45\gamma)^{-2} \ln \beta(\gamma)],$$

where $\beta(\gamma) = 0.123 + 0.813 \exp(\gamma) + 0.064 \exp(7\gamma)$.

The natural frequency of the s th mode shape of the beam with a closing crack is calculated by formula [15]

$$\omega_{cs} = 2\omega_s \omega_{os} / (\omega_s + \omega_{os}). \quad (30)$$

The analysis of the level of non-linear distortion of the time-functions being investigated was executed with the use of Fourier series:

$$F_c = \frac{a_0}{2} + \sum_{k=1}^{\infty} A_k \sin(k\omega_c t + \lambda_k), \quad (31)$$

where $A_k = \sqrt{a_k^2 + b_k^2}$, $\lambda_k = \arctg(a_k/b_k)$,

$$a_k = \frac{\omega_{cs}}{\pi} \left[\int_{t_1}^{t_2} f(x, t) \cos k\omega_{cs} t dt + \int_{t_2}^{t_3} f_c(x, t) \cos k\omega_{cs} t dt \right], \quad k = 0, 1, 2, \dots \quad (32)$$

$$b_k = \frac{\omega_{cs}}{\pi} \left[\int_{t_1}^{t_2} f(x, t) \sin k\omega_{cs} t dt + \int_{t_2}^{t_3} f_c(x, t) \sin k\omega_{cs} t dt \right], \quad k = 1, 2, 3, \dots \quad (33)$$

The instants of time t_1 , t_2 and t_3 are determined by formulae (16) and (19). Functions $f(x, t)$ and $f_c(x, t)$ in equations (32) and (33) are determined for the displacement wave shape by equations (24) and (25); for the acceleration wave shape by second time derivative of equations (24) and (25) and for the strain wave shape by equations (28) and (29) respectively.

For the estimation of the level of non-linear distortion of the displacement, acceleration and strain wave shapes, the harmonics coefficient [4] was used:

$$\chi = \sum_{k=2}^{20} A_k/A_1. \quad (34)$$

As can be seen from equation (34) on calculation of the harmonics coefficient only 20 harmonics were taken into account: further increase of their number does not lead to any essential change of the harmonics coefficients value.

It must be emphasized that if the amplitudes of concomitant modes of vibration become noticeable, the respective functions describing the wave shapes of displacement, acceleration and strain will be substantially non-periodic and it is necessary to use other approaches for the analysis of the level of their non-linearity.

5. RESULTS OF CALCULATIONS

5.1. GEOMETRICAL AND MECHANICAL CHARACTERISTICS OF THE BEAM

The geometrical characteristics of the beam are $L/h = 20$, $b/h = 1$. Crack parameters are $0 \leq a/h \leq 0.25$; $L_c/L = 0.1$ or $L_c/L = 0.5$. The mass on the end is absent ($m_L = 0$, $I_m = 0$). Young's modulus and density of the beam material as well as the ratio b/h have no influence on the relative change of the VCD under consideration (in calculations they were excepted as follows: $E = 200$ GPa, $\rho = 7800$ kg/m³, $b/h = 1$).

The results of investigation of the most sensitive vibration characteristics of wave shape non-linearity due to closing crack presence are presented; that is, the coefficient a_0 and

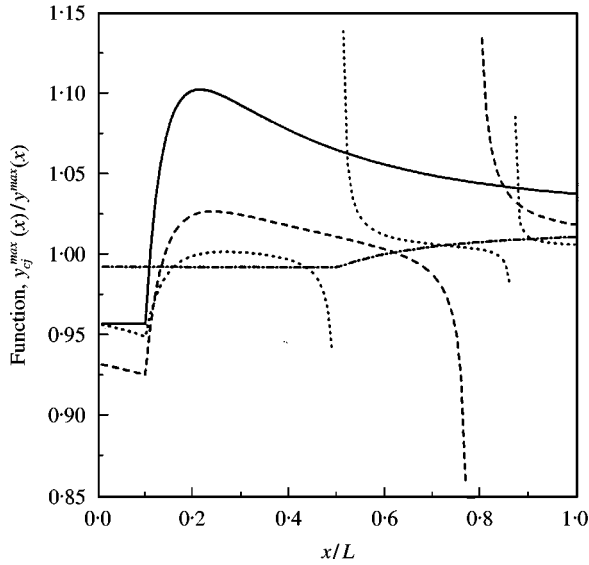


Figure 2. The change of the relative maximal deflection of the beam ($a/h = 0.25$): —, $s = 1$, $L_c/L = 0.1$; ----, $s = 2$, $L_c/L = 0.1$; ·····, $s = 3$, $L_c/L = 0.1$; - · - · - ·, $s = 1$, $L_c/L = 0.5$.

harmonics coefficient χ . Note that the relative amplitude of the second harmonic used in the study [9] as a damage characteristic is 20–30% below that of the harmonics coefficient and, therefore, is not examined here. On the other hand, a comparatively small difference between these characteristics signifies that all other harmonics do not make a great contribution to the value of the harmonics coefficient.

Figures 2–6 illustrate the change of different VCD along the beam length at $L_c/L = 0.1$ for the three mode shapes and at $L_c/L = 0.5$ for the first mode shape (in all cases $a/h = 0.25$). In these Figures and in the text, subscript “ d ” signifies the displacement, subscript “ a ” the acceleration, subscript “ cr ” the strain on the cracked surface of the beam, subscript “ int ” the strain on the intact (opposite to the crack) surface of the beam.

5.2. MAXIMUM DEFLECTION OF THE BEAM

Figure 2 shows the influence of a closing crack on the relative maximal deflection of the beam. As can be seen, the change of this characteristic is a clear qualitative symptom of fatigue damage, inasmuch as in the crack absence $y_{c_j}^{max}(x)/y^{max}(x) = 1$. The farther the crack is from the clamp, the less is the influence of the crack on the maximal deflection. The relative change of the first mode maximal deflection does not exceed 10%. For higher mode shapes it is even less. The exception in this sense presents the cross-sections in which one can observe the discontinuities of functions $y_{c_j}^{max}(x)/y^{max}(x)$. The discontinuities of respective functions are due to the fact that the co-ordinates of the nodes of vibration do not coincide with the half-cycles, while the crack is open or closed (Table 5).

It must be noted that all the functions being considered have the break in the cracked cross-section at $x/L = 0.1$ and at 0.5. The reason for this phenomenon is the fact that functions describing the vibration of a beam on the half-cycles while the crack is closed (equation (2)) and open (equation (13)) are different. This difference is due to the appearance of additional compliance in the cracked cross-section at the half-cycle of crack opening and,

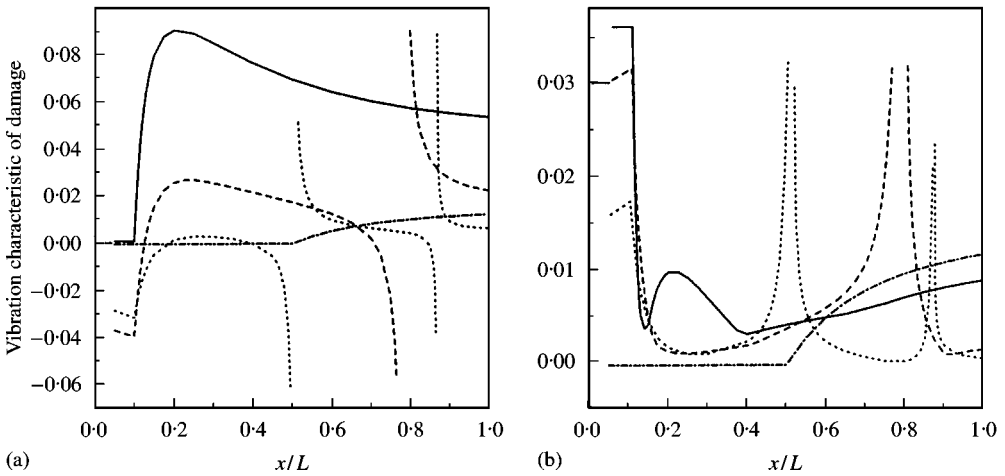


Figure 3. The relative change of the zero order (a) and harmonics (b) coefficients along the length of the beam for the displacement wave (key as in Figure 2).

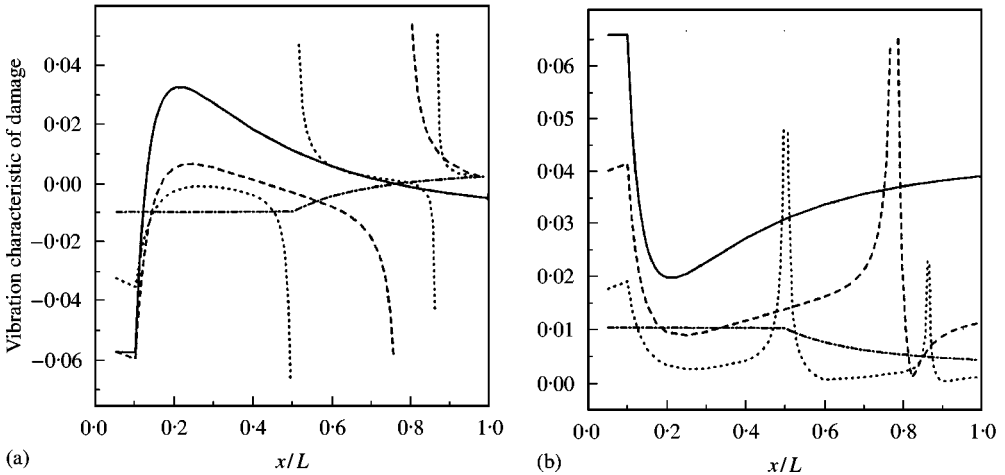


Figure 4. The relative change of the zero order (a) and harmonics (b) coefficients along the length of the beam for the acceleration wave (key as in Figure 2).

consequently, the additional angle of rotation, which causes the break of functions $y_{cj}^{max}(x)/y^{max}(x)$ (as well as other functions) in this cross-section. A similar result was reported by Yuen [16]. This peculiarity of the distribution functions can be used for the determination of crack location.

5.3. DISPLACEMENT AND ACCELERATION WAVES

The distributions of the relative change of the zero order coefficient for the displacement and acceleration waves along the beam length (Figures 3(a) and 4(a)) are qualitatively similar to the distributions of function $y_{cj}^{max}(x)/y^{max}(x)$ (in the crack absence

TABLE 5

Co-ordinates of the nodes of vibration and of the zero bending moment for the beam
($a/h = 0.25$, $L_c/L = 0.1$)

s	x/L			
	$y^{max}(x/L) = 0$	$y_{cj}^{max}(x/L) = 0$	$M^{max}(x/L) = 0$	$M_{cj}^{max}(x/L) = 0$
2	0.7834	0.7814	0.2166	0.2072
3	0.5036	0.5027	0.1324	0.1289
3	0.8677	0.8675	0.4964	0.4959

($a_0/A_1)_a = (a_0/A_1)_a = 0$). The degree of change is slightly less; up to 9% for the displacement wave and up to 6% for the acceleration wave (these estimations were executed without consideration of the functions behaviour in the neighbourhood of the nodes of vibration).

The distributions of the harmonics coefficient have qualitatively another appearance (Figures 3(b) and 4(b)). The most essential variation of the harmonics coefficient is observed in the vicinity of nodes of vibration where the respective functions reach maxima. They cannot be shown in the figures because, for example, at the second mode of vibration, the harmonics coefficient for the acceleration wave in the cross-section $x/L = 0.782433315$ reaches as astronomical value: $\chi_a = 20544.7$ (for comparison, in the cross-section $x/L = 0.782 - \chi_a = 1.48067$).

The sensitivity of zero order and harmonics coefficients for the displacement and acceleration waves drops as the crack is further from the clamp. The break of their distribution functions indicates the cracked cross-section.

Large values of zero order and harmonics coefficients in the vicinity of nodes of the second and third mode shapes are the consequence of an interesting peculiarity of physical behaviour of a cantilever beam with a closing crack, namely that of the non-coincidence of the nodes of vibration co-ordinates on the half-cycles while the crack is open and closed (Table 5). That is why, for example, if the cross-section is in the node of vibration on the certain half-cycle and consequently its displacement will be equal to zero, then on the subsequent half-cycle, the cross-section will not be in the node of vibration and the shape of total cycle will be similar to the upper (or lower) half of a sinusoid.

The level of non-linear distortion of the wave shape increases monotonically as the cross-section approaches the node of vibration causing a considerable growth of the zero order and harmonics coefficients. The discontinuity of distributions of the relative change of the zero order coefficient for the displacement and acceleration waves along the beam length (Figures 3(a) and 4(a)) is due to the fact that these functions have a different sign for the left and for the right side of the beam.

5.4. STRAIN WAVE

The distinctive feature of the zero order coefficient distributions along the beam length for the strain wave is the presence of maxima in the cracked cross-sections (Figures 5(a) and 6(a)) for all modes of vibration. As can be seen, the amplitudes of the zero order coefficient are considerable and comparable with the amplitude of the first harmonic. In this case, as in the correspondent cases of displacement and acceleration waves the discontinuity of functions at the second and third modes of vibration takes place. The reason for this

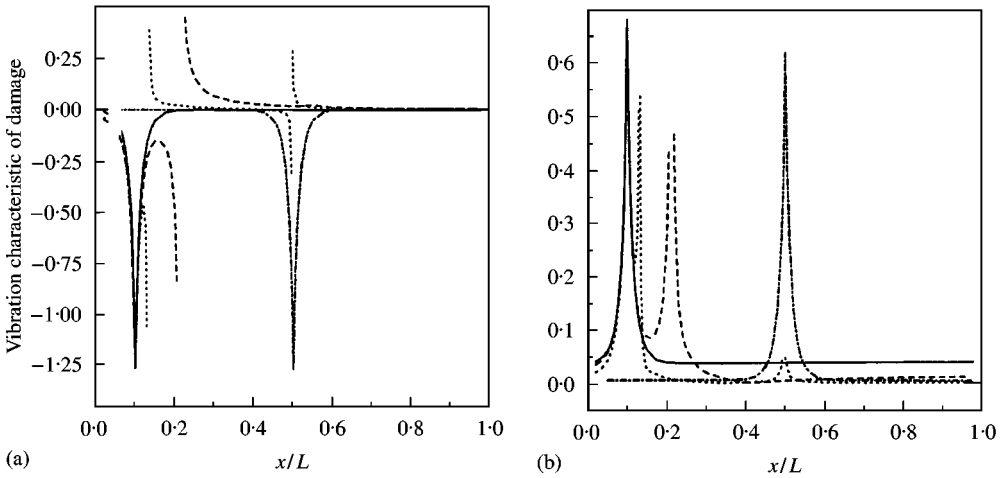


Figure 5. The relative change of the zero order (a) and harmonics (b) coefficients along the length of the beam for the strain wave on the cracked surface (key as in Figure 2).

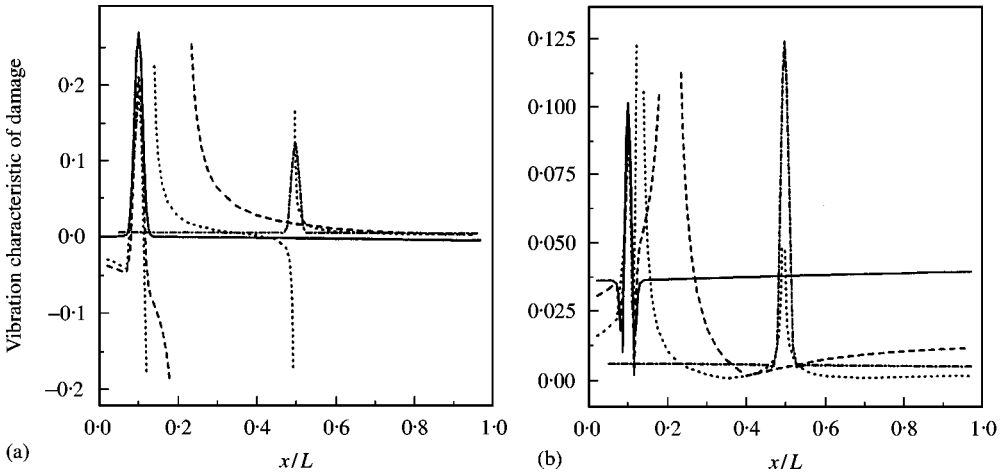


Figure 6. The relative change of the zero order (a) and harmonics (b) coefficients along the length of the beam for the strain wave on the intact surface (key as in Figure 2).

discontinuity is the non-coincidence of the cross-section co-ordinates at which the bending moment is equal to zero on different half-cycles (Table 5).

The harmonics coefficient reaches maximum values in the cracked cross-sections and in the neighbourhoods of the cross-sections with the zero bending moment (Figures 5(b) and 6(b)). Special attention must be given to the fact that the degree of harmonics coefficient variation for the strain wave on the intact surface of the beam in the vicinity of cracked cross-section increases as the crack is farther from the clamp (see Figure 6(b)). This fact qualitatively distinguishes this characteristic from all others considered.

The maxima of the functions shown in Figures 5 and 6 in the cracked cross-section are due to the predominant effect of functions $f_{\varepsilon}(x, y)$ (see section 4), which take into account the change of strain distribution on the upper (cracked) and lower (intact) surfaces along the cracked beam length.

6. COMPARATIVE ANALYSIS OF THE VCD SENSITIVITY

The analysis of the distributions of VCD along the beam length (Figures 2–6) make it possible to determine the cross-sections in which the manifestation of one or another characteristic is most significant. For instance, for the relative change of the mode shapes and the zero order coefficient for the displacement and acceleration waves such cross-sections are $x/L = 0.2$ and in the neighbourhood of the nodes of vibration. The harmonics coefficients for the displacement and acceleration waves are most sensitive in the vicinity of the clamp and nodes of vibration. The zero order and harmonics coefficients for the strain wave reach maximum values in the vicinity of cross-sections with the crack and with zero bending moment.

However, a possibility of practical implementation of the above mentioned vibration characteristics when they are measured not far from the clamp and nodes of vibration raises doubts since the level of vibrations of these cross-sections is vanishingly small. That is why Figure 7 shows the dependencies of different VCD upon the relative crack depth, the measurement of which is most realizable from a practical standpoint. The exception in this sense is only the harmonics coefficient for the acceleration wave determined in the cross-section $x/L = 0.78$ at the second mode of vibration. The amplitude of vibration of this cross-section is equal to 1.5% of maximum amplitude of vibration of the beam. It must be noted that the zero order coefficient for the strain wave on the cracked surface (it is shown without regard for the sign of the original function) as well as the harmonics coefficient χ_{cr} (the absolute value is 2 times less than the zero order coefficient; the corresponding curve is not shown in Figure 7) are practically independent of crack size. Because of this, the noted characteristics discussed are unfit for the damage estimation. At the same time, similar characteristics determined on the intact surface of the beam are closely dependent on the crack growth. Figure 7 also shows the dependencies of the relative change of natural

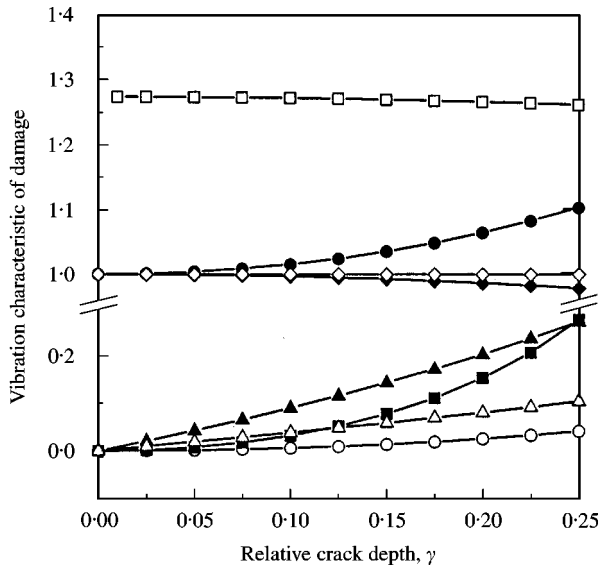


Figure 7. The effect of crack depth on the relative change of the VCD ($L_c/L = 0.1$) —●—●—, $F = y_{cj}^{max}(x)/y^{max}(x)$, $x/L = 0.2$, $s = 1$; —○—○—, $F = \chi_{a0}$, $x/L = 1$, $s = 1$; —■—■—, $F = \chi_{a0}$, $x/L = 0.78$, $s = 2$; —□—□—, $F = (a_0/A_1)_{cr}$, $x/L = 0.1$, $s = 1$; —▲—▲—, $F = (a_0/A_1)_{int}$, $x/L = 0.1$, $s = 1$; —△—△—, $F = \chi_{int}$, $x/L = 0.1$, $s = 1$; —◆—◆—, $F = \omega_c/\omega$, $s = 1$; —◇—◇—, $F = \omega_c/\omega$, $s = 3$.

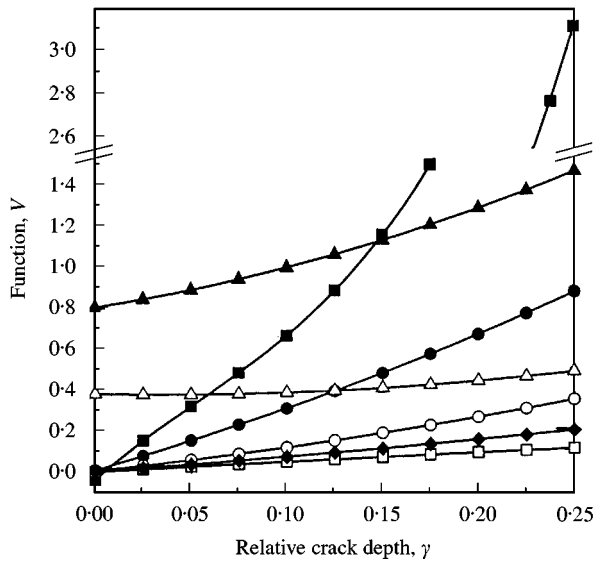


Figure 8. The effect of crack depth on the velocity of functions $F(\gamma)$ change (key as in Figure 7).

frequencies of the beam upon the crack depth. As can be seen, the influence of the crack on the natural frequencies is small in comparison with the other VCDs.

In the present work, the sensitivity of the VCD means the measure of the respective vibration characteristic change under the unitary variation of damage size. As such, when a measure was used the velocity of functions $F(\gamma)$ change describing the relationship between the relative change of the VCD and damage size:

$$V(\gamma) = \partial F(\gamma) / \partial \gamma. \quad (35)$$

Comparative analysis of the VCD efficiency was based on the comparison of functions $V(\gamma)$ at the certain value of argument.

As can be seen from Figure 8, none of the VCD presented in Figure 7 is most sensitive over the entire range of crack depths being investigated. The most sensitive characteristics in the range of small cracks were found to be the zero order and harmonics coefficients for the strain wave on the intact surface of the beam in the cracked cross-section. The sensitivity of the relative change of functions $y_{cj}^{max}(x)/y^{max}(x)$ and harmonics coefficients for the acceleration wave are high in the second half of the crack size range. However, the possibility of practical determination of the latter characteristic is very problematical.

As a whole, VCD stated here possess sufficient sensitivity to detect small cracks. However, as pointed out above, these characteristics were determined in the specially selected cross-sections in which they are most sensitive. In its turn, the co-ordinates of these cross-sections are dependent on the crack location. Thus, for the optimal use of the VCD being considered the crack location should be known. Theoretically, the VCD (with the exception of natural frequencies) provide such a possibility; the crack location can be judged by the break of the distribution function, of the corresponding VCD along the beam length or by the maximum of this function. Unfortunately, the determination of such a function in practice is very labour-consuming and not always a feasible process.

7. CONCLUSIONS

The method of consecutive (cycle-by-cycle) solutions of the free bending vibration problem for a beam with a closing crack was obtained; that is the mode shape amplitudes of the cracked beam were determined on a limited number of cycles of its vibrations.

The method made it possible to define the important qualitative features of the cracked beam behaviour, namely: the growth of concomitant modes of vibration in the process of crack opening and closing; and each half-cycle of the beam vibration is characterized by the non-recurrent set of amplitudes of concomitant modes of vibration. The latter may signify that the rigorous steady state solution of such class problems does not exist even if the damping is taken into account. The amplitudes of concomitant modes of vibration are heavily dependent on the crack depth.

The distribution functions of the VCD based on the evaluation of the level of non-linear distortions of the displacement, acceleration and strain waves over the beam length were determined for three mode shapes. A closing crack essentially causes non-linearity of these distribution functions; this fact may serve as a diagnostic indication of damage. The distinctive features of the behaviour of distribution functions in the neighbourhood of cracked cross-section (break or maximum) indicate the crack location. The quantitative estimation of the functions changes as crack growth making it possible to determine the size of crack. In such a manner, the problem of damage diagnostics can be fully solved based on the analysis of the distribution functions.

The zero order and harmonics coefficient for the strain wave determined in the neighbourhood of a cracked cross-section on the intact (opposite to the crack) surface of the beam were determined to be the most sensitive from the VCD being investigated.

REFERENCES

1. A. IBRAHIM, F. ISMAIL and H. K. MARTIN 1990 *Journal of Sound and Vibration* **140**, 305–317. Identification of fatigue cracks from vibrating testing.
2. A. RYTTER, R. BRINCKER and P. H. KIRKEGAARD 1992 *Fracture and Dynamics, Paper No. 37, Department of Building Technology and Structural Engineering, University of Aalborg*. An experimental study of the modal parameters of a cantilever.
3. S. M. CHENG, A. S. J. SWAMIDAS, X. J. WU and W. WALLACE 1999 *Journal of Sound and Vibration* **225**, 201–208. Vibrational response of a beam with a breathing crack.
4. P. F. RIZOS, N. ASPRAGATHOS and A. D. DIMAROGONAS 1990 *Journal of Sound and Vibration* **138**, 381–388. Identification of crack location and magnitude in a cantilever beam from the vibration modes.
5. I. BALLO 1998 *Journal of Sound and Vibration* **217**, 321–333. Non-linear effects of vibration of a continuous transverse cracked slender shaft.
6. R. RUOTOLO, C. SURACE, P. CRESPO and D. STORER 1996 *Computers and Structures* **61**, 1057–1074. Harmonic analysis of the vibrations of a cantilevered beam with a closing crack.
7. S. L. TSYFANSKY and V. I. BERESNEVICH 1998 *Journal of Sound and Vibration* **213**, 159–168. Detection of fatigue cracks in flexible geometrically non-linear bars by vibration monitoring.
8. D. AFOLABI 1987 *Proceedings of the Fifth International Modal Analysis Conference, London, England*, 491–495. An anti-resonance technique for detecting structural damage.
9. A. P. BOVSUNOVSKY and V. V. MATVEEV 2000 *Journal of Sound and Vibration* **235**, 415–434. Analytical approach to the determination of dynamic characteristics of a beam with a closing crack.
10. W. M. OSTACHOWICH and M. KRAWCZUK 1991 *Journal of Sound and Vibration* **150**, 191–201. Analysis of the effect of cracks on the natural frequencies of a cantilever beam.
11. H. TADA, P. PARIS and G. IRWIN 1973 *The Stress Analysis of Crack Handbook*. Hellertown, PA: Del Research Corporation.
12. G. P. CHEREPANOV 1974 *Mechanics of Brittle Fracture*, Moscow: Nauka (in Russian).

13. R. REID PARAMETER and B. MUKHERJI 1974 *International Journal of Fracture* **10**, 441–444. Stress intensity factors for an edge-cracked strip in bending.
14. A. P. BOVSUNOVSKY and A. G. KRATKO 1998 *Journal of Testing and Evaluation* **26**, 31–37. The shape of mechanical hysteresis loops for metals under harmonic loading.
15. S. TIMOSHENKO, D. H. YOUNG and W. WEAVER Jr 1974 *Vibration Problems in Engineering*. New York: John Wiley; fourth edition.
16. M. M. F. YUEN 1985 *Journal of Sound and Vibration* **103**, 301–310. A numerical study of the eigenparameters of damaged cantilever beam.